CHAPTER 16

INJECTION SYSTEM

16.1 OVERVIEW AND MAIN PARAMETERS

16.1.1 Introduction

Injection into LHC is performed in the combined experimental and injection insertions IR2 and IR8. The transfer line TI 2 brings the beam to a point ~150 m left of IP2 for injection into Ring 1 and TI 8 delivers the beam ~160 m right of IP8 for injection into Ring 2, as this IP is displaced 11.22 m from the injection point. The transfer lines with the injections are described in more detail in [1].

A schematic layout of the injection region near IP8 is given in Fig. 16.1. In both insertions the beam approaches the LHC from outside and below the machine plane. The beam is directed by a last series of dipoles, already located in the LHC tunnel, towards a series of five Lambertson type septum magnets which deflect the beam horizontally by 12 mrad under the outer ring. A series of four MKI kicker magnets deflects the beam vertically by 0.85 mrad onto the orbit. In order to allow a proper injection setup with pilot bunches and to protect the LHC in case of malfunctioning of the injection kickers, an injection beam stopper, TDI, is placed 15 m upstream of the superconducting recombination dipole D1, supplemented by an additional shielding element, TCDD, 3 m upstream of D1. The protection against injection errors is further complemented by two collimators, TCLI, near the superconducting quadrupole Q6 on the other side of the insertion.

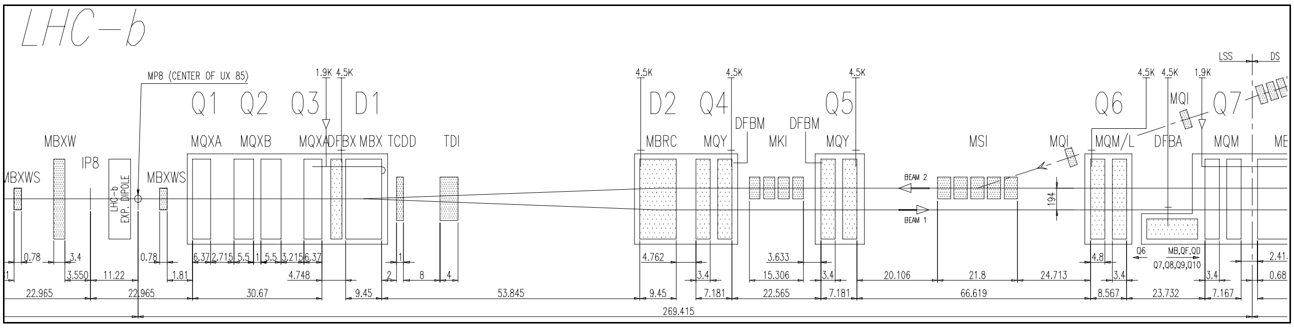

Figure 16.1: Schematic layout of the injection region right of IP8

The geometrical layout and arrangement of MSI, MKI and TDI/TCDD among each other and, within a few mm, also with respect to the adjacent machine elements is identical for both injections. However, despite being based on the same design criteria, the optics varies between IR2 and IR8 due to the displaced interaction point in IR8. The vertically defocusing quadrupole Q5 between the MSI and the MKI provides, through its kick enhancement, about one quarter of the required total vertical deflection. It should be noted that, although this is not apparent in the schematic layout above, the size of the Q6 cryostat is reduced to leave space for beam to be injected. The precision of the injected beam's position with respect to the LHC closed orbit is specified to be less than $\pm 1.5\sigma$, including SPS closed orbit errors at extraction, ripple and drifts of power supplies and injection kicker ripple. Further parameters can be found in the descriptions of the individual components.

16.1.2 Scope and Chapter Organisation

Each of the following sections is devoted to a major injection specific equipment, following the order seen by the beam to be injected – septa, kickers, and stoppers. This is followed by a discussion of the injection related beam instrumentation. A further section discusses the relations between the injection and other machine systems and the requirements put upon them. The description of general accelerator-wide systems or services like vacuum is restricted to the extent that a sufficient degree of self-containment for the component under consideration is produced; for a more in-depth treatment the reader is referred to the relevant chapters. A discussion of the auxiliary injection collimators, TCLI, can be found in the chapter describing the collimation system. The transfer lines collimators, TCDI, are only briefly mentioned as to their protection function for the injection septa. Even though their main role is to protect LHC elements against beam arriving with too large transverse or angular offsets, the main discussion about them is deferred, owing to their physical location, to the chapter describing the injection transfer lines.

16.2 INJECTION SEPTA

16.2.1 Machine Layout and Main Parameters

Five septum magnets (MSI) of two different types (MSIA and MSIB) deflect the beam to be injected horizontally by 12 mrad under the outer ring. For injection into Ring 1 the septa are located in RA23 between Q6 and Q5, and similar for Ring 2 in RA87. MSIA and MSIB magnets differ in the septum thickness (the distance of the holes for the circulating beams from the pole) and the coil configuration and, consequently, the field in the gap. In the direction of the beam to be injected three MSIB magnets are followed by two MSIA magnets and including the inter-magnet gaps, the whole system stretches over 21.8 m. The main parameters of the injection septum magnets are given in Tab. 16.1.

Table 16.1: Main parameters of the injection septum magnets

	MSIA	**MSIB**	
Septum core length	4000	4000	mm
Coil core length	3650	3650	mm
Core width	734	734	mm
Core height	529	529	mm
Gap height	25	25	mm
Septum thickness	6	15.5	mm
Number of coil turns	16	24	-
Number of coil layers	4	6	-
Number of turns per layer	4	4	-
Electrical coil resistance at 20 °C	10.9	16.4	mΩ
Inductance	10.2	23.7	mH
Dissipated power	10.6	15.9	kW
Water flow per coil	7.9	11.8	l/min
Coil pressure drop	5	5	bar
Design current	950	950	A
Nominal magnetic field in the gap	0.76	1.13	T
Magnet weight	9800	9900	kg

16.2.2 Magnet Design

The magnets were designed and built in a collaboration between CERN and the Institute for High Energy Physics (IHEP) in Protvino, in the framework of the contribution of the Russian Federation to LHC [2, 3]. A view of the connection front face of both magnets is given in Fig. 16.2 and Fig. 16.3 shows a side view.

The laminations are punched from 1.0 mm thick steel sheets with a 10 µm thick Fe_3O_4 layer as electrical insulation. The magnet yokes are an all-welded construction and are assembled from different half cores, the so-called septum core and the coil core. The septum core comprises circular holes for the circulating beams, thus avoiding the need for the careful alignment of the usually wedge-shaped septum blades used in classical Lambertson magnets. The septum core is longer than the coil core to reduce the stray field extending from the field gap to the circulating beam holes. The coil core holds the single pancake coil.

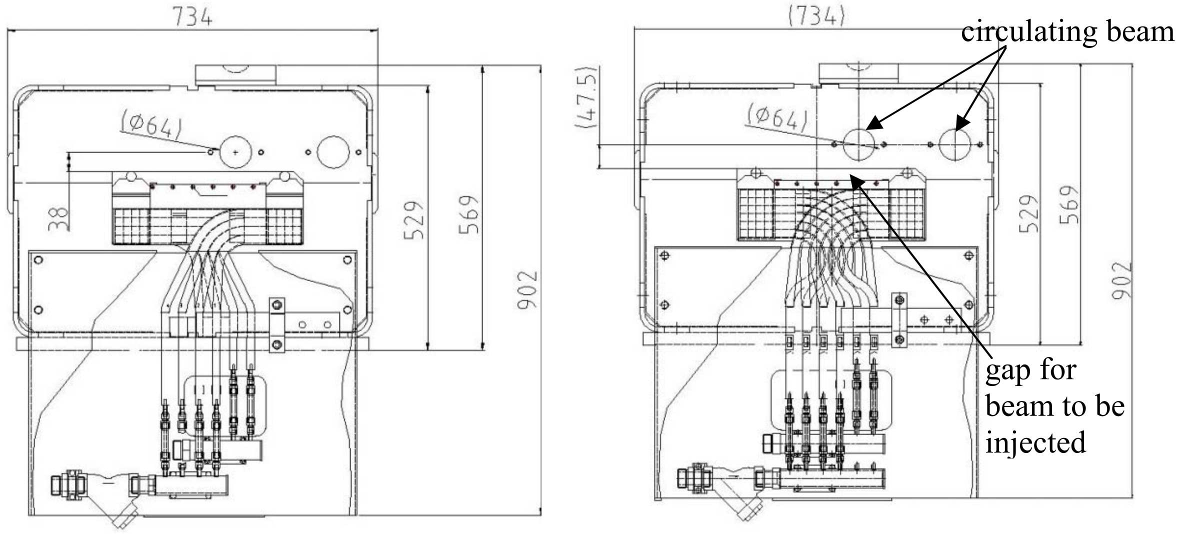

Figure 16.2: MSIA (left) and MSIB (right) connection front face view

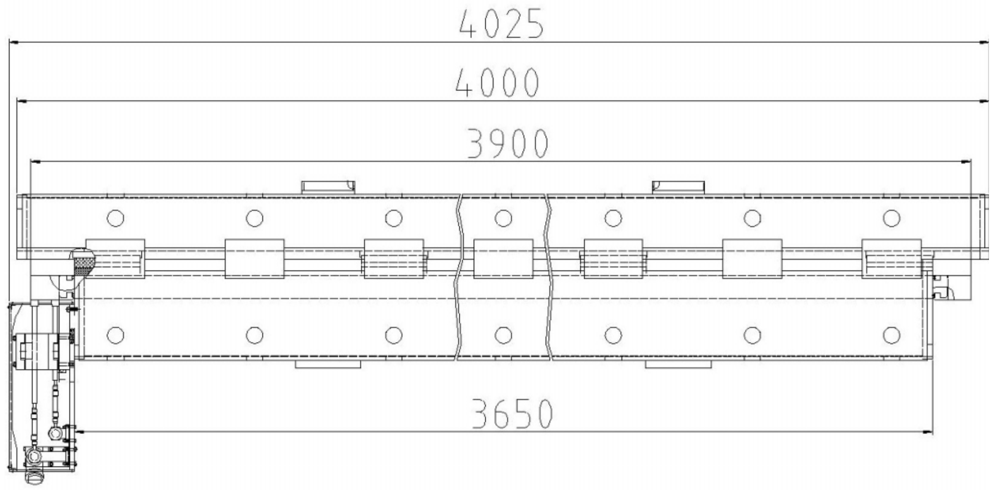

Figure 16.3: MSI side view

The coils are made from a 15 mm wide OFHC square copper conductor with a circular cooling hole of ≈ 4.5 mm diameter, insulated with glass fibre tape and impregnated using a radiation resistant resin. Each coil water outlet carries a thermo-switch to prevent overheating of the coil by switching off the MSI power converter if there is a defect in the cooling circuit. The trip temperature on the switch is 65°C and control is made through the magnet surveillance system,

16.2.3 Vacuum System

The vacuum system of the MSI magnets has to fulfil several stringent requirements. The beam holes in the septum cores have a diameter of 64 mm. The mechanical vacuum system tolerances including their alignment and the alignment of the magnet in general, must be such as not to reduce the available aperture significantly. The circulating beam must be shielded against the stray field leaking from the core into the septum holes, with a measured dipole component of the order of 10 Gauss [4]. The vacuum chambers for the circulating beams should be bakeable to 250°C in situ without heating the magnet yokes to more than 120°C. The combination of all constraints like the beam hole diameter, alignment tolerances, magnet tilt angle, aperture requirements and the need for bake-out led to the choice of a mumetal chamber with an inner diameter of 56 mm and a wall thickness of 0.9 mm [5]. The stray field remaining for the smaller chamber which had been envisaged before was calculated to be of the order of 0.1 Gauss [6].

To reduce the outgassing rate of the chambers to meet the ultra high vacuum requirements, a bake-out at 250 °C using special heaters [7] for at least 24 hours is made [8]. These heaters comprise three layers: a stainless steel heating strip in the centre surrounded by two insulating polyimide films. Wrapped around the chamber the total thickness of such a heater is 0.3 mm. A reflective aluminised polyimide film is wrapped on top of the heater sandwich. Special thermal insulation precautions have been taken to reduce the heat load on the magnet yoke, keeping its maximum temperature below 120 °C.

The inner surface of the chambers is copper coated using electrochemical deposition with a fluid circulation technique which is required due to the length of the tubes (~5 metres). A current delivered by a pulsed power supply is transmitted into the electrolyte through a copper electrode surrounded by a platinum coated titanium grid. The tube is placed in a vertical position to avoid bending problems and a pump drives the electrolyte through the mumetal tube [9]. Preliminary tests demonstrate that a copper thickness of 0.5 mm can be achieved with good resistive characteristics [10] (values of up to 0.85 mm have been obtained). For aperture reasons a baseline thickness of 0.4 mm was chosen [11]. Finally, the circulating chambers are NEG (Ti-Zr-V Non Evaporable Getter) coated to improve the pressure and thus the background for the experiments and to avoid electron cloud build up.

Both ends of the chambers for the circulating beams are fitted with DN200CF flanges (316LN) which are welded after insertion of the chamber in the magnet. The chambers are centred in the septum holes using one stainless steel ring (304L) in two parts, spot welded in the centre. This not fully penetrating spot weld must be made before the copper deposition to avoid the destruction of the copper layer during the welding and to allow the recovery of the magnetic properties by the high temperature thermal treatment (1050°C). Further centring is obtained through two other stainless steel rings (304L) mounted at the ends of the chambers. These three rings, welded on each chamber, must pass through the magnet hole. Two copper coated (0.4 mm) extensions in 316L and are welded at each end of the mumetal chamber to allow the welding of the temporary and the final flanges. The manufacturing tolerances of the mumetal tubes could lead to unacceptable gaps between the tubes and the apertures machined in the flanges. To keep the assembly gap constant and thus to preserve the reliability of the welds between the mumetal and the flanges, the tube ends will be recalibrated (plastically deformed by inserting a high precision machined profile).

The chambers of the beam to be injected are made from 304L stainless steel with an inner diameter of 22 mm and a wall thickness of 1 mm. Mounting is achieved by special form pieces along the gap and welded strips at the ends. The chambers are baked at 85°C for 24 hours to minimise the outgassing onto the circulating beams' NEG coated chambers. The bake-out is performed using the special sandwich heaters developed for the circulating chambers.

A special 300 mm long modular pumping port equipped with a 60 l/s pumping speed ion pump is fitted in the 450 mm inter-magnet gap. All inter-magnet gaps will be equipped with pumping ports to provide the required differential pumping between the chambers for the circulating beams in the order of 10^{-10} mbar and the chambers for the beam to be injected of the order of 10^{-7} mbar, while permitting a reasonably fast exchange of a magnet in case of failure. However, the pumping port configurations are specific to each inter-magnet gap so that the spare magnet could only be equipped after identifying the faulty magnet.

Prototypes fulfilling all requirements mentioned above have been made at CERN and a Functional Specification has been written for the series production [12].

16.2.4 Aperture and Alignment Issues

The effective apertures in the septa are determined by the vacuum chambers, the magnet alignment, the beam sizes and orbit offsets in these locations. To optimise the available aperture without making the vacuum design too magnet specific, the magnets will be tilted with respect to the machine plane and the MSIA and MSIB groups precision aligned with different chamber axis offsets. A qualitative plot of the vertical beam trajectory and the beam envelope, showing the two groups of septa (MSIA left and MSIB right), is shown for the circulating and injected beams in IR2 in Fig. 16.4. For the circulating beam a $9.8\sigma_y$ beam envelope is shown, including 21% beta beating, 27% parasitic dispersion, ±4 mm orbit error and ±2 mm mechanical and alignment tolerance (the mechanical tolerances of the chamber are treated as effective position errors of the beam) . For the injected beam, a $5\sigma_y$ beam size is plotted, including 21% beating and ±1.5 mm mechanical and alignment tolerance.

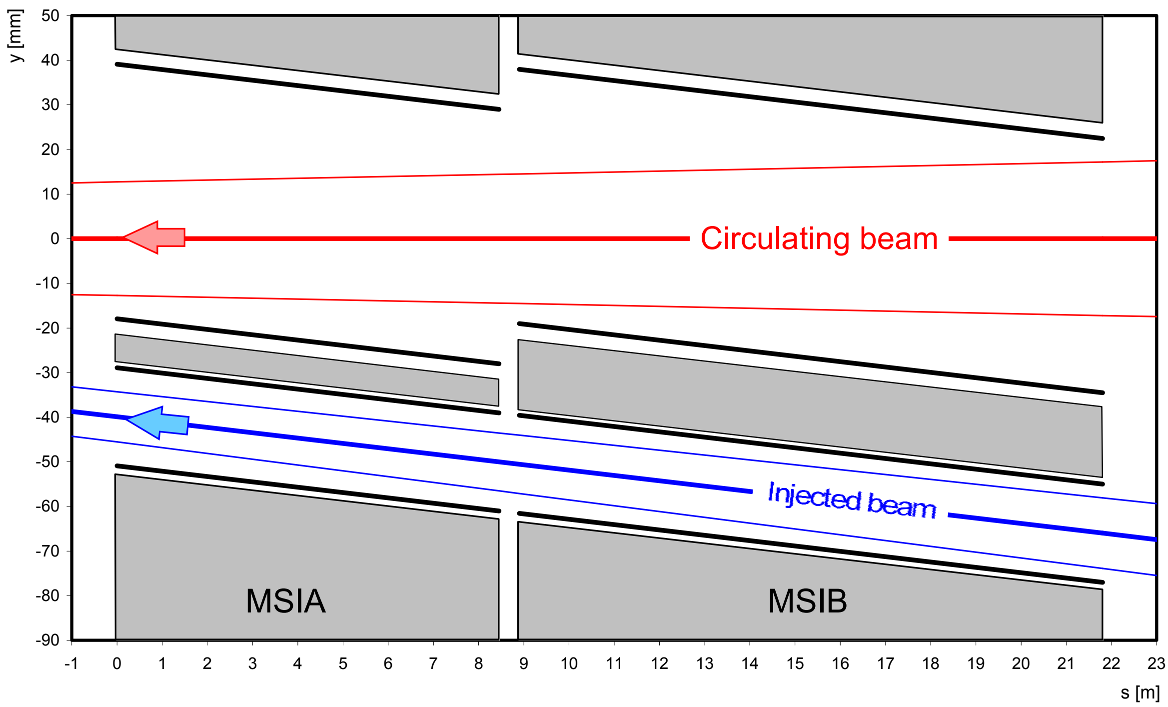

Figure 16.4: Vertical beam trajectory and envelope through the injection septa in IR2

16.2.5 Protection

The last TCDI collimator in each transfer line will be placed just upstream of the first injection septum magnet in order to protect the septa against misdirected beam [13, 14]. Together with the other transfer line collimators it will also protect elements further downstream in the LHC. It will probably consist of a fixed graphite mask of about 3 m length and 5 – 6 σ aperture. The detailed design has not been finalised at the time of writing.

16.2.6 Powering and Control

The MSIA and MSIB septa of one injection line are powered in series using a 1000 A, 200 V power converter, with a nominal current of 950 A. The current precision required ($\Delta I/I_{nom}$) is $\pm 1 \times 10^{-4}$ with an interlock level set at around $\pm 5 \times 10^{-3}$ to prevent damage to the LHC in the event of a converter trip prior to the SPS extraction. The septa will be slowly pulsed for each injection with a rise time of several hundred ms and a similar length flat top. A digital controller (Function Generator Controller, FGC), as used for other LHC magnets, controls and supervises the converter. In the event of a trip or instability prior to injection, the present response time of 5 ms of the surveillance system means that the maximum possible orbit deviation will be ~6 - 7σ in the horizontal plane, which is at the limit of causing problems for the LHC collimation system. It may be necessary to reduce this figure by upgrading the surveillance system for these converters.

16.3 INJECTION KICKERS

16.3.1 Overview and Machine Layout

The injection kicker system (MKI) comprises four fast pulsed magnets per injection. The magnets are housed in a separate vacuum tank comprising both beam pipes which has been recuperated from the LEP separators. For injection into Ring 1 the magnets are located in RA23 between Q5 and Q4, for Ring 2 injection in RA87. The pulse generators and part of the power and control electronics are located in the adjacent underground gallery, UA23 in for IR2 and UA87 for IR8. The transmission cables pass through two existing holes previously used for wave-guides. Fig. 16.5 gives the layout (plan view) around the LHC injection kickers in IR8 and Fig. 16.6 a cross section.

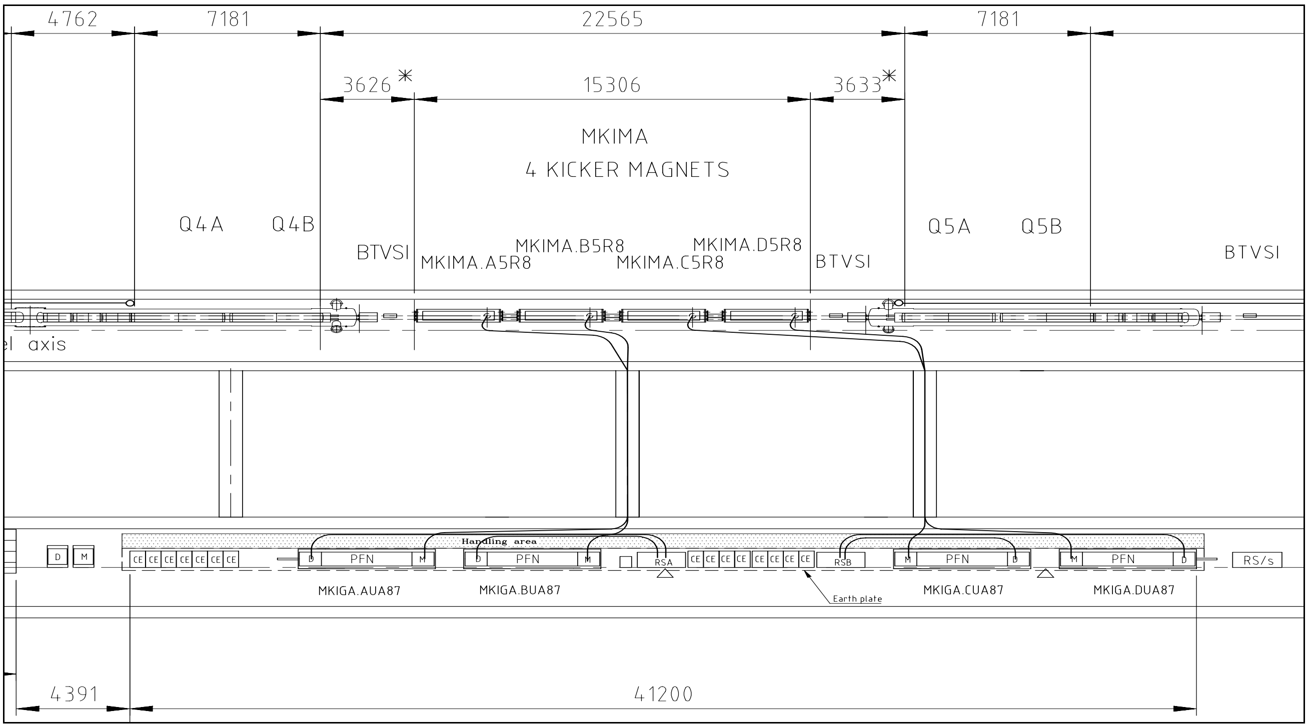

Figure 16.5: Injection kicker layout right of IP8 (plan view)

16.3.2 Main Requirements and Parameters

The beam to be injected approaches the kicker system from below at an angle of 0.85 mrad, requiring a total integrated dipole field of 1.2 Tm for deflection onto the central machine orbit. To limit the emittance blow-up at injection, reflections and flat top ripple of the field pulse must stay below ± 0.5% – a very stringent requirement. The pulse repetition time is imposed by the SPS acceleration cycle, 18 s in case of 3-train extraction. The LHC will be filled with 12 batches of 5.84 µs or 7.86 µs duration, to be deposited successively on the machine circumference, with 11 gaps of 0.94 µs in between them to account for the injection kicker rise time. One final gap of 3.0 µs accounts for the fall time of the injection kickers and allows also for the rise time of the beam dumping kickers. The main parameters are summarised in Tab. 16.2.

Table 16.2: Main MKI system parameters

Item	**Value**	**Unit**
Number of magnets per system	4	-
System deflection angle (4 magnets)	0.85	mrad
∫ B dl	0.325	Tm
Magnet beam aperture (diameter)	38	mm
Characteristic impedance	5	Ω
Operating charging voltage (PFN)	54	kV
Field flat top ripple	< ± 0.5	%
Field flat top duration	up to 7.86	µs
Field rise time 0.5 %-99.5 %	0.9	µs
Field fall time 99.5 %-0.5 %	3.0	µs
Yoke length	2.650	mm
Magnet length (mechanical)	3.400	mm

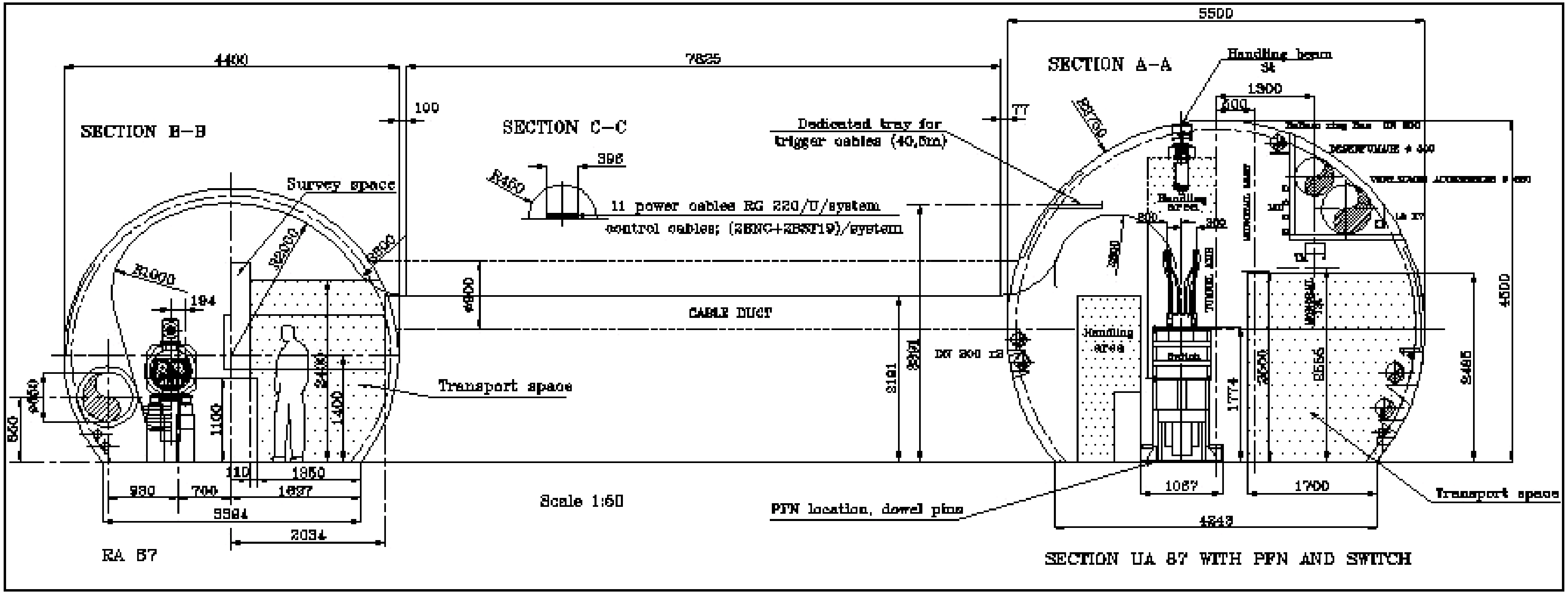

Figure 16.6: Cross section of tunnel section RA87 and underground gallery UA87 around the MKI

16.3.3 Equipment Description

Overview

The schematic circuit diagram of the injection kickers is given in Fig. 16.7. Each magnet is powered by a separate pulse-forming network (PFN). Two PFNs are charged simultaneously from one resonant charging power supply (RCPS). To be able to vary the pulse duration a main switch (MS) and a dump switch (DS) are needed, one at either end of the PFN. A carefully matched high bandwidth system is necessary to fulfil the stringent pulse response requirements. The system is therefore composed of a multi-cell PFN and a multi-cell travelling wave kicker magnet, connected by a matched transmission line and terminated by a matched resistor [15]. To achieve the required kick strength a low characteristic impedance of 5 Ω was chosen.

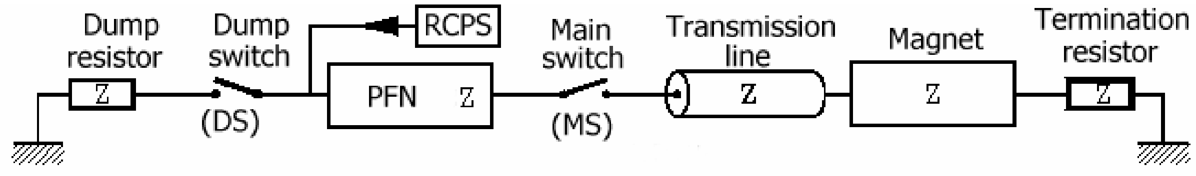

Figure 16.7: Schematic circuit diagram

The design voltage is 60 kV, as in most SPS kicker installations, allowing the use of several proven components such as transmission lines, connectors and termination resistors. The voltage on the magnet is half of the PFN voltage - allowing for overshoot, the design voltage of the magnet is 35 kV. The major components are discussed below in more detail.

Magnet

Each kicker magnet consists of a series of 33 cells: a compromise between bandwidth and cost. Fig. 16.8 shows a cross section of one magnet cell, with matching capacitors mounted between a high voltage and a ground plate. The plates are spaced by three ceramic-metal insulators, which together form an independent cell assembly. To achieve a characteristic impedance of 5 Ω within the space constraint of the 540 mm diameter tanks, two ceramic plate capacitors with 210 mm diameter each and contoured rims have been used leading to a nominal self-inductance and capacitance per cell of 101 nH and 4.04 nF, respectively, including the plate end effect.

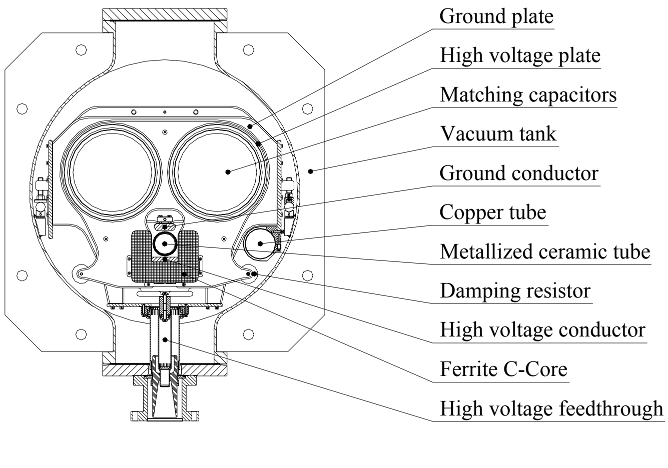

Figure 16.8: MKI magnet cross section

For stability reasons the capacitors are made of a monolithic class 1 ceramic with relative permittivity of about 75. The electrodes are formed by painted and then baked silver layers. In order to avoid surface flash-over problems and to achieve reliable operation at full voltage, the voltage holding capabilities have been extensively studied using finite element computer codes to simulate the geometry of the transition between the connecting plates and the capacitors. The critical electrical contact is ensured by toroidal spring contacts all around the capacitor rims and an accurate rim geometry. Careful design of the mechanical components (distances and radii) was needed to maintain the electrical fields below 5 MV/m. Deflectors have been added to eliminate the electrical field at the triple junction. High voltage and ground plates have been electro-polished.

The viability of using ceramic capacitors in ultra high vacuum has been demonstrated through outgassing tests. Good vacuum quality of some 10^{-10} mbar in operation is ensured by bake-out at 300°C, vacuum firing and heat treatment in air on most of the parts of the magnet. To be bakeable the magnet has been made of stainless steel, aluminium being unsuitable for such temperature cycles. Low inductance damping resistors have been connected in parallel with the cells. They have been specially developed for UHV compatibility and consist of two counter-wound Kanthal® wires on a ceramic rod.

In order to reduce beam impedance while allowing a fast field rise time, the beam passes through a ceramic pipe with silver stripes on its inner wall. The stripes provide a path for the image current and screen the ferrite yoke against beam induced heating [16]. The stripes are directly connected to the standard vacuum chambers of the machine at one end and via a decoupling capacitor of 300 pF at the other, using the ceramic pipe itself as dielectric. The pipe is made from a 3 m long extruded ceramic tube with a wall thickness of 4 mm. The stripes are produced using a photochemical technique similar to printed circuit boards but complicated by the difficult access to the inside of the tube. Two layers of silver paint are first applied uniformly inside with bake-out at 800°C after each layer. A mask is then held against the inner wall by vacuum while UV light is passed through the pipe. The 200 mm of the tube which extends outside the magnet has its is outer surface uniformly painted silver and the inner surface has the stripes, thus giving the required capacitance between each stripe and the outer layer. The latter is connected to the metallic beam tube of the machine. The other beam traverses the vacuum tank inside a copper chamber.

The ferrite cores are made from high permeability and high resistivity NiZn type, 8C11 grade, and have a C-configuration to allow earthing of the coaxial HV cable input connection and the output connection to the terminating resistor [17]. In addition to their magnetic properties which are specially adapted to this application, they exhibit very good vacuum performance after appropriate treatment [18].

Again, in order to obtain a fully bakeable design, the conductors are made from stainless steel. The shape of the ground conductor has been optimised in order to provide a homogeneous field without having to machine shims on the ferrites.

PFNs

PFN type generators are used to produce rectangular pulses with very low ripple. The top part of the current pulse in the prototype magnet is shown in Fig. 16.9.

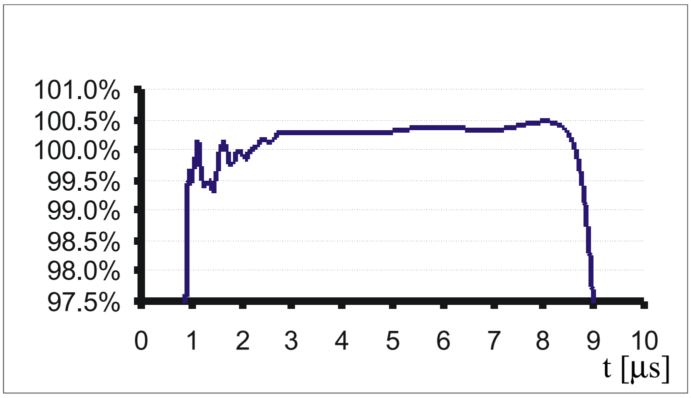

Figure 16.9: MKI prototype current pulse shape (top part)

Since experience had shown that adjusting individual inductances of a PFN would not lead to a flat top ripple smaller than about ± 1 % [19] the inductances are wound as a continuous straight and rigid coil with constant and high precision pitch to guarantee the same self inductance and mutual coupling coefficient for all cells. A characteristic impedance of 5 Ω with adequate frequency response requires cell inductances of less than 1 μH. As such small inductances cannot be built cost effectively with the required high precision, two networks of 10 Ω impedance are connected in parallel.

Conduction losses along the coil, resulting in droop of the top of the magnetic field pulse in the kicker magnet, are compensated for by grading the values of the capacitors such that they increase in value from the MS end to the DS end of the PFNs [20]. Component values leading to an acceptable field rise time, fall time, and ripple, have been chosen in an iterative way, using the PSpice optimiser [21]. In order to obtain a realistic transient response, most known parasitics were modelled in the simulation of the electric circuit as well as the voltage and frequency dependency of components. For optimum pulse response the component values of the end cells differ from those of the central cells.

The PFNs are housed in a metallic tank and insulated with silicone fluid. The capacitors are mounted vertically and in individual coaxial housings. The two straight and continuous copper coils are tightly wound around a threaded glass reinforced epoxy cylinder to ensure a precise and constant geometry along the coil. A series of holes through the cylinder allows connections to be made to the capacitors mounted below and in line with the coil. Each coil is shielded by a screen connected to the coaxial housing of the capacitors. The coils are connected in parallel, and then to the switches via a common coaxial "plug-in" feed-through.

HV Switches

Main and dump switches have been designed for minimum size and easy maintenance. They use three-gap thyratrons of types CX 2003 and CX 2503, installed in independent tanks with isolating transformers for heaters, reservoirs and grid biasing. These switches are mounted directly onto the PFN to save space and cost as in the SPS injection kicker installation [19]. The post-pulse period is only critical for the last of the 12 injection pulses. The DS is only required for this last pulse.

Transmission Lines

The pulse is transmitted from the PFNs to the magnets through 10 parallel RG220 type coaxial cables of 50 Ω impedance and 35 m total length each. The conductors are drawn from electrolytic copper and low density polyethylene of high purity is used as dielectric. The cable can be exposed to an integrated radiation dose of at least 10^6 Gy. Cable ends are terminated by moulded high voltage connectors as already in use in the SPS.

Matching Resistors

Both matching resistors are assembled from ceramic-carbon discs mounted in a low inductance coaxial housing and insulated with silicone fluid. This type of resistor is extensively used at CERN, but the adjustment to the required value and the resistance stability remain an issue for this very precise application.

Safety Aspects

To reduce the fire hazard, the transmission cables are flame retardant and free from halogens and sulphur in accord with CERN Safety Instruction IS23 and IEC Standard 332-3. The resonant charging power supplies, PFNs, switches and terminating resistors are insulated by a silicone fluid (dimethylsiloxane polymer) with high ignition point. Conventional smoke detection is installed in the pulse generator areas.

The whole circuit has been designed so that personnel cannot come into contact with high voltage. All components are contained in grounded metallic containers or racks. The disconnection of HV cables or opening of the containers is not possible without tools, and the rack doors are locked by key and equipped with micro switches fitted to disconnect the primary power supply and discharge all high voltage capacitors and other stored charges before allowing access. The x-rays produced during the operation of the thyratrons are shielded by their metal housing. Therefore, no access limitation is required during the tests and conditioning. Yellow flashlights, however, are installed in the tunnel and gallery and indicate when the system is operating.

Vacuum Issues

Each tank is equipped with two 400 l/s ion pumps and two 1000 l/s titanium sublimation pumps, all recovered from the LEP separators and re-installed using the previous layout. The tank will be baked up to 300 °C using the separator heating jackets.

Due to the overall size of the vacuum tank the other ring also passes through the tank and for impedance reasons this has to pass through a copper tube which has 60 mm inner diameter. NEG coating has been added for vacuum and electron cloud reasons. The ion pumping of this tube is ensured to a level of 40 l/s by the conductance at each end through RF fingers and to a level of 200 l/s by holes located at 1/3 and 2/3 of the tube for impedance reasons. The NEG coating will be activated during the bake-out of the tank at 300°C.

Each tank is equipped with a Pirani and two Bayard-Alpert gauges (SVT type); only one is cabled and the other serves as spare. The ion pumps also provide the vacuum interlock for the high voltage of the kicker generators by means of a hardwired signal from the pump power supply.

There are vacuum valves at each end of the group of four kicker magnets but no individual vacuum valves between each magnet for cost reasons. An intervention on one of the tanks therefore requires a new bake-out in situ of the whole set of magnets. This takes about 8 days, and must be followed by about four days of reconditioning.

Exploitation and Maintenance Issues

Regular maintenance will be focused on the thyratron switches. Their lifetime under the conditions of use in the LHC is estimated to between five and eight years. Regular adjustments will be required. Based on experience with the SPS injection kicker system and depending on the budget available for preventive maintenance, the expected down-time due to the MKI system should be of the order of 10 to 30 hours per year, not counting the time for access to the underground galleries.

Faults

Note that a more thorough discussion of injection kicker faults and their impact is contained in Sec. 16.4.1, with only some basic information given here for self-consistency.

Owing to their nature as gas tubes the thyratron switches are liable to possible self-firing (“erratic pulses”) or not firing when required (“missing pulses”). Non firing of the kicker system can also occur when no RF prepulses are received. In this case the beam to be injected continues straight onto the injection beam stopper (TDI).

In the case of erratic firing of one kicker generator, all kickers are immediately triggered and then beam will be swept over the full deflection range with some 20 bunches escaping the TDI and propagating to the auxiliary injection collimators or the cleaning system [22]. This type of fault is expected to occur a few times per year. It should be noted that the PFNs are only charged 2 ms before injection in order to limit the time during which such errors can occur. After injection the kickers are switched off.

More severe consequences can result from a flash-over inside a kicker magnet, particularly if it occurs in some specific cells. In the worst case almost a full batch can just escape the TDI and end up on the cleaning collimators. From experience with the prototype magnet and several improvements introduced in the series this event is estimated to occur less than once per ten years of operation [23].

16.3.4 Control System

Overview

The kicker control system, schematically shown in Fig. 16.10, comprises three independent entities: one for the control of the equipment state (ON, OFF, STANDBY…), one for the control of the injection process (timing system and operational setting management) and one for the control of the fast signal acquisition and interlock logic (protection of the equipment and of the machine), each implemented in an appropriate technology.

The injection process is composed of two consecutive stages which are repeated for each injection. First a slow stage divided into two phases: a 1000 ms long charging phase of the primary capacitor bank followed by a 2 ms long resonant charging phase for charging the PFNs with a pulse-to-pulse reproducibility of 0.1%. Then a fast stage of 10 µs duration for synchronisation of the timing system with the circulating and to-be-injected beams, triggering of the thyratron switches, discharging of the PFNs and generation of the magnetic pulse.

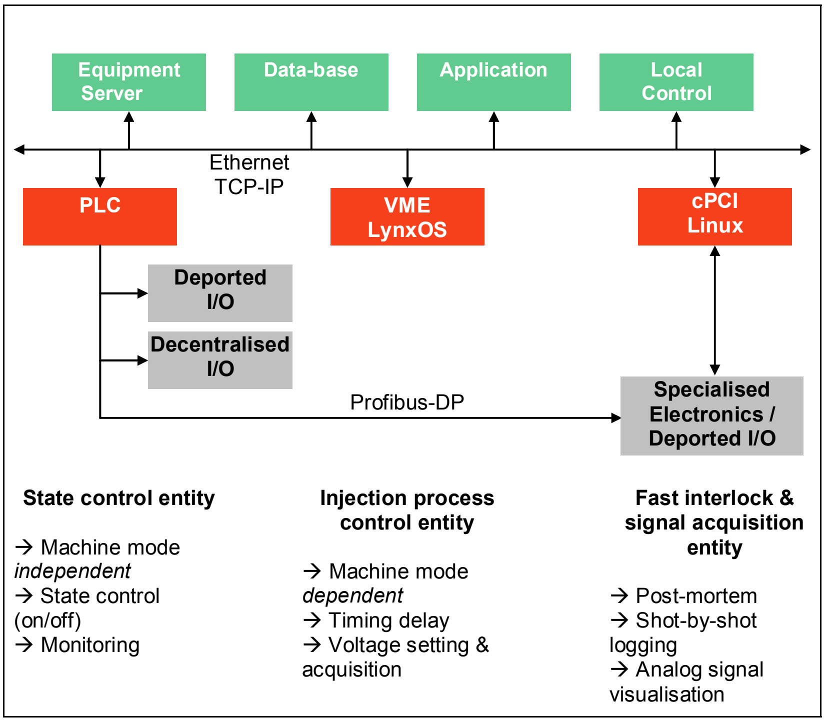

Figure 16.10: MKI control system architecture

State Control

The state control is based on a SIEMENS S7-400 master programmable logic controller (PLC), which is linked through two identical PROFIBUS-DP segments to the various equipment controllers (resonant charging power supply controller, thyratron heater controller, terminating resistor controller, pulse generator controller). They are connected either as deported I/Os or as decentralised I/Os when low-level intelligence is required. A third PROFIBUS-DP segment is used to interface to the resources common to the two generators of one injection, like electrical distribution and temperature measurements. The master PLC is connected to the Ethernet TCP/IP network for communication with the application layer. Modelling of the different controller functionalities at the master level is performed through dedicated functional software blocks. MKI state transition management and state acquisition are implemented through a finite state machine running in the master PLC level.

Injection Process Control

The injection process control consists of a LynxOS VME PowerPC front-end computer including four 1 ns resolution digital delay modules. These are used for trigger pulse generation in phase with injected and circulating beams and for fine timing adjustment, one 16 bit DAC/ADC module for kick strength settings and measurements and one standard LHC timing module (CTX1) for synchronisation with the machine timing. The management of the different operational settings during the injection process is based on a real-time task running in the front-end.

To ensure high reliability of the injection process, the thyratron triggering system is based on a fully redundant architecture up to the primary side of the thyratron trigger transformers. A comprehensive fast monitoring system supervises at each injection pulse the correct operation of the complete system and allows fault tracing on the various active elements (resonant charging system, thyratron erratic or missing pulses, magnet or transmission line sparks, terminating resistor open or short-circuit, timing synchronisation failure, etc.). In addition, a pre-triggering system ionises the gas tubes 500 ns prior to injection in order to reduce the thyratron turn-on delay and to optimise the turn-on jitter.

Fast Interlock Control

The fast interlock logic, built from specialised electronics, continuously surveys all the critical parameters of the injection process and upon detection of a failure either inhibits the injection process or reduces the impact of the failure and inhibits further injections.

Equipment state failures occurring up to 2 ms before injection inhibit the charging process and the SPS extraction. In this case, beam is dumped in the SPS. If the failure occurs in the 2 ms window before injection, the charging process in progress will not be stopped but the LHC injection and SPS extraction be inhibited until the reason of the failure has been removed.

The injection process can be inhibited up to 250 ns before injection. It has to be noted that there is no possibility to stop the magnetic pulse rapidly once it has been started since the system is not equipped with clipper switches at present. The shortest magnetic pulse length is 3 μs, followed by a fall time of 3 μs.

Remote analogue visualisation of injection related waveforms is based on the OASIS system [24].

Exploitation and Maintenance Related Issues

All control electronics are located in the underground gallery near the pulse generators. Personnel making interventions have at their disposal a complete set of low level monitoring and diagnostic tools. These are available in the galleries, in the surface buildings and also remotely for a continuous surveillance of the whole installation. During machine operation, access to the galleries is required only in case of a hardware failure of an electronics module. All operational parameters, like timing settings, interlock thresholds, etc., are remotely controllable. Each intervention on the installation, e.g. a remote setting change, is logged. Control of critical parameters is password protected.

Preventive maintenance is limited to the verification and re-calibration of electronics modules and the replacement of electromechanical components like relays or fans.

16.4 INJECTION BEAM STOPPER AND SHIELDING

16.4.1 Injection Beam Stopper

Layout

The injection beam stopper (TDI) is used for injection setting-up and machine protection in case of a malfunction of the injection kickers. For maximum efficiency it is located ~70 m downstream of the injection kickers at a vertical phase advance $\mu_v = 90^\circ$, 15 m upstream of the superconducting recombination dipole, D1. It is complemented in its protection function by the supplementary shielding device TCDD, described further below. The TDI is housed in a 5 m long vacuum tank recuperated from the LEP separators.

The active part of the TDI consists of two absorber jaws, ~4.2 m long, one above the beam and one below [25]. The upper jaw intercepts beam arriving from the transfer line which has not been sufficiently deflected by the injection kickers, the lower jaw receives circulating beam kicked away from the orbit. The jaws can move vertically in a range of ±2 - 60 mm from the nominal beam axis by means of two dc servo motors per jaw. The side view of the tank, including the motor assemblies, the ion pumps and the support feet, is given in Fig. 16.11.

Each jaw consists of a sequence of segments of absorbing materials mounted in an aluminium frame. Eighteen hexagonal boron nitride (hBN) blocks, each 157.7 mm long, are followed by one 600 mm long aluminium block and one 700 mm copper block. All segments have a cross section of 58 mm width and 54 mm height. The evacuation by conduction of heat deposited is eased by means of flexible copper strands between the jaws and the tank.

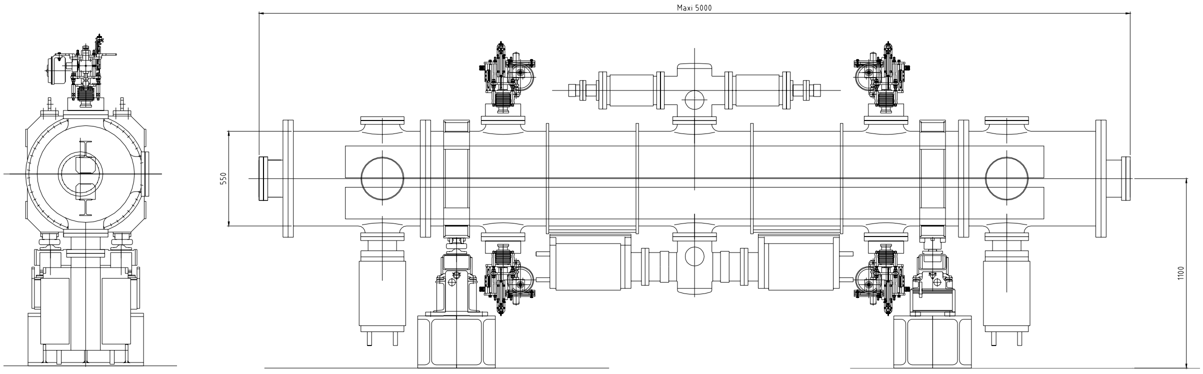

Figure 16.11: TDI cross section and side view

Mechanical Parameters

Table 16.3: Main mechanical TDI parameters

Item	Value	Unit
Tank length	5000	mm
Jaw stroke	± 2 - 60	mm
Jaw flatness	0.3	mm
Jaw position resolution and reproducibility	20	µm
Jaw speed	1	mm/s
Weight per jaw	200	kg

The drive mechanism entails a mechanical backlash of 70 µm. Jaw inclinations as high as 33 mrad are mechanically possible in case one motor is in the innermost position (2 mm from the nominal beam axis) and the other one fully retracted (at 60 mm), but the maximum operational range needs still to be defined.

Impedance Aspects

To reduce beam impedance the hBN blocks are coated with 3 µm of titanium and the aluminium block with 10 µm of copper, like the aluminium frame. To provide a path for the image current and mask off the tank cavity against the beam a complex-shaped 1.5 mm thick stainless steel (316LN) beam screen with 300 µm copper coating is located on each side of the jaws. This beam screen limits both the disturbance to the beam and the local heating caused by losses,

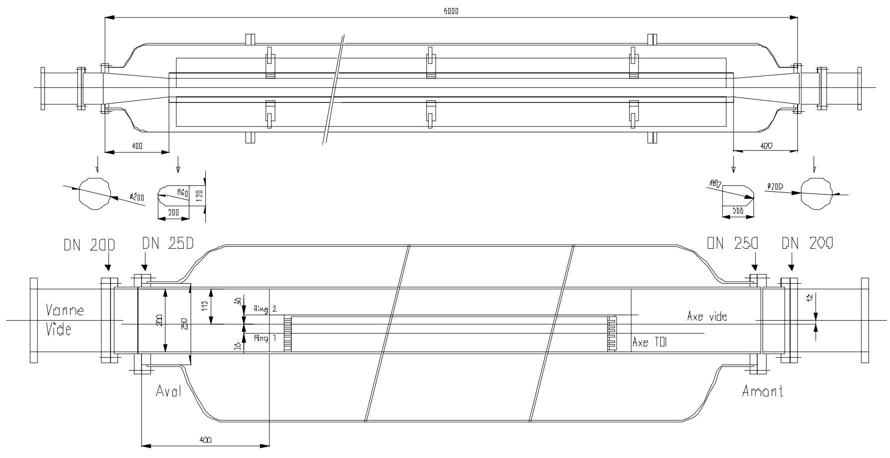

Figure 16.12: Schematic longitudinal cross-section of the TDI with beam screen

Cone shapes at both extremities ensure a smooth transition to the adjacent vacuum chamber segments. The mechanical and electrical connection to the mobile jaws is made with sliding contacts. A longitudinal cross section of the TDI and a cross section of the TDI in IR2, showing the beam screen, are given in Fig. 16.12 and 16.13, respectively.

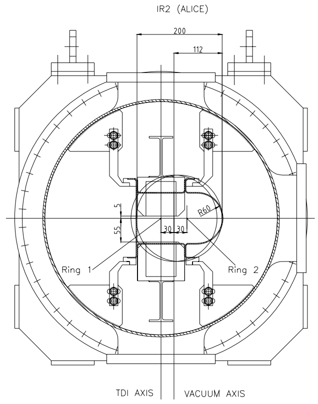

Figure 16.13: TDI cross section at IR2

Vacuum Aspects

Owing to the proximity to the experiments, the background from residual gas scattering in the TDI must be kept small. Two ion pumps of 400 l/s each and two titanium sublimation pumps of 1000 l/s each provide an efficient pumping speed of 1600 l/s in total. The expected residual pressure inside the beam screen is 10^{8} mbar during normal operation after an in-situ bake-out. Sufficient vacuum transparency of the beam screen, at about 10 % of its surface, is provided through a large number of quasi-irregularly positioned holes which measure 11 × 2 mm.

The suitability of hBN for this quite novel application has been verified through extensive testing of both the mechanical resistance and the vacuum aspects [26]. Prior to mounting, the material undergoes a heat treatment at 400 °C under vacuum. After installation and following any intervention, the tank is baked out at 200 °C using heating jackets. To improve removal of gas emanating from the absorber during bake-out and after interception of significant amounts of beam, the absorber segments contain machined slits and are mounted with 5 mm gaps. The aluminium jaw frame will be heated directly by a resistive wire (stainless steel) mounted inside a groove on both sides of the frame, isolated by ceramic rods. During bake-out the motor drives will be protected from overheating by temporary air cooling. Temperatures will be monitored by PT100 sensors located on each jaw, with an interlock level set slightly above 200 °C to prevent deterioration of the mechanical properties of the aluminium.

The vacuum system has been designed to cope with the outgassing during normal operation, i.e. with a jaw temperature between 20 and 35°C. As thermal outgassing increases dramatically with temperature, a vacuum degradation of the order of 10 will be incurred for a temperature increase of 50°C. Operating temperatures of higher than 50°C will therefore possibly lead to gas density levels exceeding those required near the experiments.

Fault Cases Considered

According to the initial design specification the various circumstances leading the TDI to intercept beam have been investigated and grouped in cases [22], with the same total kick strength seen by the beam. Operational (i.e. intentional) uses of the TDI were considered to imply the repetitive use of single bunches without leading to quenches of the superconducting dipole D1 located downstream, accidental or emergency uses were to proceed from the assumption of full batch intensity, without causing damage to D1.

In case 1 the kick strength is zero. Besides the during commissioning and during re-adjustment of the injection before each fill this could happen when the SPS extraction was launched but the LHC suddenly turned out not to be ready to receive beam. It could also be caused by a missing trigger to the MKI. This could happen several times per year. In this case the beam hits the upper jaw at about 30 mm from the lower edge.

Case 2, the beam sweep occurs when the rise or fall slope of the kicker pulse coincides with the passage of beam to be injected or with the circulating beam. This could occasionally occur as a result of wrong kicker timing, either due to an internal or external reason, or a pre-fire of one of the modules. Several precautions are taken to make this a relatively rare event. The pulse generators are only charged 2 ms before an injection, making the time when a breakdown in the thyratron gas tubes could occur quite short. As soon as one kicker module has pre-fired the other modules are also triggered. In this case close to 100 bunches are distributed on the TDI with various offsets from the jaw edge.

The also quite rare case 3 refers to one of the four MKI modules not firing. In this case the beam hits the upper jaw at about 3.5 mm from the lower edge.

Case 4 is an internal flashover on one of the MKI magnets. The consequences are particularly bad when the flashover occurs in any of a range of 8 out of the 33 cells. In this case beam would just miss the TDI and approximately 90 % of an injected batch could hit the collimators. To reduce the consequences the dump switches will be fired upon detection of such a flashover, terminating the pulse and reducing the intensity leaking into the LHC machine by a factor of 2. Based on the prototype results and several other improvements implemented in the series kickers this case is expected to be a very rare event, happening less than once per 10 years of operation [23].

Protection Performance

The TDI/TCDD/D1 ensemble has been simulated and optimised using FLUKA [27]. The material of the TDI sandwich construct lumps up to about 15 interaction lengths. Considering the TDI alone for case 1 leads to no quench, even at highest intensities. Without the additional shielding provided by the TCDD described in 16.4.2, case 4 would approach the limit for producing damage to the D1 coil for a nominal full batch and surpass it slightly for ultimate intensity. The TCDD reduces the energy deposition in the coil by about two orders of magnitude and thus excludes damage to D1 under all circumstances. Its presence is of course also beneficial for the cases 2 and 3, so that quenching D1 can probably be avoided for the sweep case for nominal intensity.

To ensure this protection the TDI must be set very close to the beam for injection. Details of possible impact of beam missing the TDI or leaking from it onto other machine components are discussed in [22]. Two additional collimators, positioned at a phase advance of $\mu_v \approx \pm 20^{\circ}$ from the TDI, near Q6 on the other side of the insertion, and set at the same aperture will extend the protection of the TDI in case of phase errors.

Structural Considerations

The mechanical performance of the TDI has been studied using the numerical code ELSE which is based on the Spectral Element Method (SEM) [28]. The structural behaviour of all of the hBN blocks was modelled up to 80 μs after the absorption of a full batch at ultimate intensity for a centred beam load, in order to identify the most critical one. The highest temperature increase and radial thermal gradients are located in the first three blocks, with a maximum $\Delta T = 638$ °C in the third one. The most stressed blocks are the first five, while the last blocks show a more uniform stress field.

Since hBN is an orthotropic material, the maximum stress criterion was selected to assess the structural performance of the absorbing core; this criterion is more conservative than the Stassi (or generalized Von Mises) criterion usually adopted for graphite. The components of the dynamic stress tensor were evaluated at each time step and each node of the SEM model. The ratio between these values and the rupture stress was calculated and a maximum value of 0.32 was found, which gives a stress safety factor of three at ultimate intensity. The most stressed volume is concentrated around the beam axis, though other parts of the block are subjected to relevant stresses due to the propagation and reflection of elastic stress waves.

Because the beam may be intercepted at various distances from the free edge of the absorbing segments (the “impact parameter”), numerical simulations were performed for the most critical third hBN block with a varying impact parameter. For the chosen stress criterion, the maximum stress is approximately constant for the different beam positions and the stress ratio close to the above-mentioned value of 0.32.

The use of fine-grained polycrystalline graphite was investigated as an alternative to hBN. Due to the higher thermal expansion coefficient and lower mechanical resistance, higher stresses ratios were found. Based on the Stassi criterion, a maximum stress ratio of 0.76 was estimated for a centred beam load, giving a safety factor as low as 1.3. Worse values are expected for off-centre loadings, which substantiates the choice of hBN.

Downstream of the hBN blocks, the estimated temperature rise after interception of one full batch at ultimate intensity is 150°C in aluminium and 190°C in copper. These values, together with the very low thermal gradients, are estimated to be low enough not to require a dedicated structural analysis.

Dose Rates

Tab. 16.4 shows the estimated dose rates of the TDI under the assumption of 10^{15} protons being dumped per year, as a function of the number of years in operation and the cool-down time. The values scale with the intercepted intensity and almost saturate after 10 years of operation. The TDI activation is low enough to allow human intervention around the vacuum tank, and, after an appropriate cool-down time, also on the jaws itself. This holds a fortiori for the TCDD described in 16.4.2.

Table 16.4: Estimated TDI dose rates in mSv/h when intercepting 10^{15} protons per year

Cooling time	*Contact dose at*	**Operation time**	
		1 year	**10 years**
1 min	*Core*	112	120
	Tank	16	16
1 day	*Core*	0.5	0.6
	Tank	0.09	0.09
1 month	*Core*	0.08	0.12
	Tank	0.02	0.03
1 year	*Core*	0.02	0.05
	Tank	0.005	0.015
10 years	*Core*	0.003	0.02
	Tank	0.0003	0.002

Operational Aspects

After dumping the previous circulating beam and prior to the next injection, the TDI jaws are closed to a nominal position of $\pm$ 8.5σ (about ±4.3 mm). After injection the TDI jaws are retracted.

Owing to its basic design purpose the TDI core is not actively cooled. The thermal inertia of the TDI jaws allows the absorption of single SPS bunches of ultimate intensity (1.7×10^{11} protons per bunch) during commissioning and adjustment of injection every 18 s for about 8 hours consecutively. For a few consecutive SPS cycles the TDI is able to intercept a full batch of $4 \times 72 = 288$ bunches at ultimate intensity. Normally this case should not occur as further extraction of intense beam towards LHC should be inhibited after one error, until the source of the fault has been removed. The temperature in the TDI absorbers will be monitored and fed back to the SPS extraction system to prevent over heating and thus mechanical deformations leading to loss in TDI precision or even severe malfunctioning.

16.4.2 Supplementary Shielding for D1

The TDI alone is sufficient to prevent damage to D1 in practically all cases of injection kicker malfunction. To prevent damage even in the worst MKI flashover case where a full batch just grazes the TDI jaw, an additional shielding element (TCDD) is placed about 3 m upstream of D1. This also improves the TDI performance for other fault cases.

Its absorbing element consists of two copper jaws placed inside a vacuum tank. In the closed position, they form a cylindrical core ∅ 70 mm × 1000 mm with a rectangular opening of 30 × 50 mm and rounded corners. This assembly shadows the D1 coil with a beam clearance ~15σ. A side view of the TCDD, along with a cross section, is given in Fig. 16.14. Longitudinally, the jaws are wedge-shaped to avoid particle streaming, as shown schematically in Fig. 16.15.

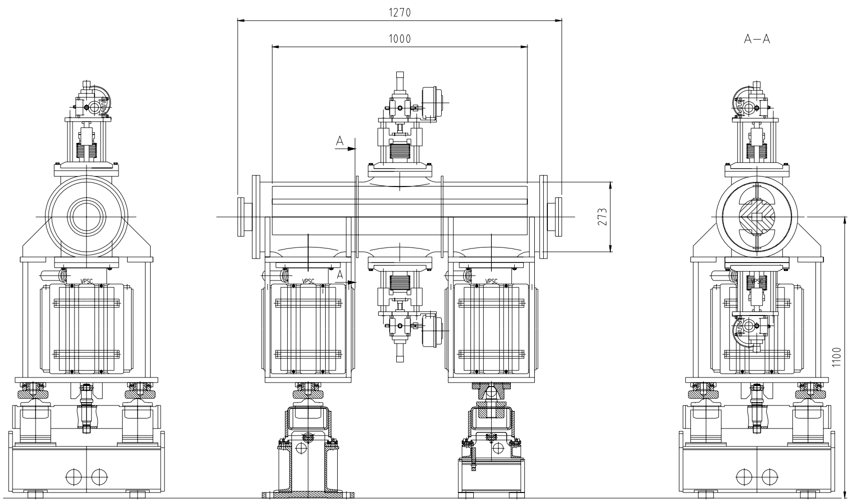

Figure 16.14: TCDD side view and cross section

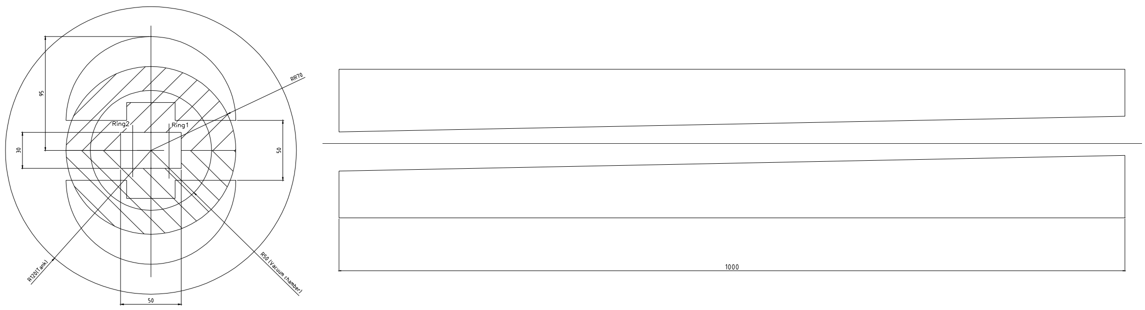

Figure 16.15: TCDD absorber cross section and side view

In IR8 the jaws are always fixed in the closed position and no motorisation is provided. In IR2 the jaws can be opened by ±50 mm to provide appropriate aperture for the ALICE Zero Degree Calorimeter once injection is terminated.

The design of several TCDD sub-components (motorisation, supports) is based on that of the TDI. One ion pump of 400 l/s is mounted on a simple steel tank of 1270 mm length and 273 mm diameter. As 200°C is the maximum bake-out temperature acceptable on the tank, the jaws will be baked directly up to 250°C using the same heaters as in the TDI. The TCDD is not cooled and should see no direct beam.

16.5 BEAM INSTRUMENTATION

16.5.1 Overview

The beam instrumentation around the injection systems is a direct continuation of the transfer line systems in TI 2 and TI 8. Therefore the functional specifications for the transfer lines [29, 30] have been used in the design choices for these systems. A schematic overview of the instrumentation in the injection region is given in Fig. 16.16. Only instruments forming an integral part of the LHC rings are described below; elements being part of the transfer lines (grey shaded in contrast to black filled symbols) and physically separate from the rings are described in Volume 3.

The transfer line beam position monitors (BPMI) allow steering of the beam up to the entry of the septum magnets. The BPMs around the injection elements are standard ring BPMs installed on the superconducting quadrupoles, details of which can be found in Sec. 13.1. Luminescent screens (BTVI) using the optical transition radiation effect (OTR) are used to determine the transverse beam sizes and centre of gravity upstream and downstream of the major injection elements and provide complementary position information during the setting up and steering of the injection. Standard SPS type beam-loss monitors (BLMI) are used to localise the losses linked to the injection process. Installed instruments can cope with the full variety of LHC beams. For proton operation, the intensity varies from a single pilot bunch, namely 5×10^{9} protons, to 4 batches of 72 bunches with up to 1.7×10^{11} protons per bunch.

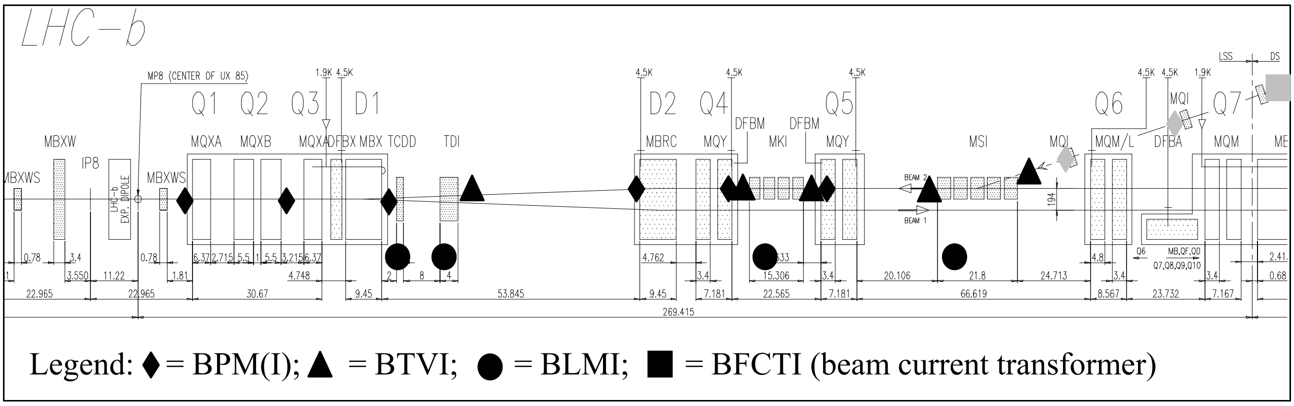

Figure 16.16: Schematic view of injection related instrumentation (case of injection near IP8)

16.5.2 Beam Loss Monitors

The beam-loss monitors around the injection systems are of the SPS type. The ionisation chambers and acquisition system are described in [31, 32]. Acquisitions are triggered using SPS timing events pre-programmed at the correct time in the SPS elementary cycle. The beam-loss server allows returning data either in raw ADC units or calibrated in units of mGy. The calibration of the whole acquisition chain is done with an external source.

Dynamic Range and Precision

The dynamic range to be considered for the LHC beam corresponds to a factor 10^{4} if the losses scale linearly with the total intensity. The acquisition cards have 12 bit ADCs which is insufficient to cover this dynamic range. It will therefore be necessary to use the on-board gain switches providing gains between 1 and 2.5×10^{4}.

16.5.3 Beam Profile Monitors

The BTV mechanisms are of a new type with respect to the existing SPS version, as they have to allow the movement of three different screen holders (one of them being empty) within a very confined space between the transfer line and the LHC ring vacuum chambers. The first physical screen that can be inserted into the vacuum chamber is made of a foil of alumina (Al_2O_3) for low intensity use and the second of titanium for OTR observation at intensities $>10^{11}$ particles. The second screen can alternatively be equipped with a carbon foil believed to withstand even ultimate LHC intensity. The round foils have a diameter of 65 mm and cover therefore the entire acceptance of the vacuum chamber, making it possible to use them for calculating the beam position over a very wide range. Depending on the choice of fixed optics in front of the BTV camera, a part of the screen can be selected for digitisation. This defines in the end the resolution in the range between 60 µm to 120 µm per pixel. The resolution can be user-defined, owing to the trade-off between resolution and screen coverage.

As the aperture near the injection region is restricted, measurements of the beam size and beam position (centre of mass) obtained from the transverse beam profile monitors are mandatory to steer the beam and minimise the injection oscillations. BTV monitors are inserted at the entrance and exit of the MSI and MKI to optimally position the beam inside those devices and check their correct functioning. One monitor is placed in front of the TDI inside the LHC tunnel to obtain correct initial conditions for the trajectory on the first turn.

BTV Acquisition

The acquisition of beam profile data is based on high-resolution CCD cameras linked to a newly developed BTV acquisition card giving a two-dimensional image with a digitisation of 300 × 400 pixels. The screen position, filters and an external lamp can also be controlled from the same VME module. All monitors provide two-dimensional information. For normal batches the integrated beam spot must be made available. By directing the light emitted by the passage of the beam through the screen towards a fast profile acquisition system, bunch-by-bunch profiles (X and Y projections) are possible at selected monitors [33]. The last option requires the installation of further BTV tanks that are not part of the present layout.

Reproducibility on Position and Size Measurements

Measurements on an existing SPS BTV tank [34] have shown that the reproducibility on the measurement of beam size and centre of mass for a spot size equivalent to that of the LHC beam is very good. The beam position (centre of mass) acquired over 10 consecutive screen movements changes by around 100 µm peak-to-peak and the beam size is determined to within 1% which is well within the specifications. Even better results are expected with the newly designed BTV tank if special care is taken during the alignment of the BTV screens.

Acceptance

The BTVs should, if possible, cover a large fraction of the vacuum chamber aperture. The profile monitor optics and readout should be adjustable to cover either a large area at the expense of a loss in accuracy, or to cover a significantly smaller area optimised for optics and emittance measurements. During the first commissioning of the lines, the profile monitors should be tuned to cover the largest possible fraction of the aperture.

16.5.4 Software

The low-level software for all instrumentation systems in the transfer lines and thus also around the injection systems is based on a common front end software architecture [35] which provides a set of generic structures allowing the production of graphical user interfaces for operations as well for expert applications used during the setting-up of these systems.

16.5.5 Interlocks

The beam loss monitors in the transfer lines and in the injection region are part of the SPS extraction interlock. Whenever the rates exceed a given preset threshold, extraction from the SPS is inhibited for the following cycles. A machine operator has the possibility to reset this interlock in order to perform tests and, if required, improve the steering of the line or of the extraction channel. An automatic reset mechanism may be applied to prevent useless machine downtime in case of a spurious problem, as is already done in the SPS ring. There are also ideas to incorporate a software interlock to inhibit further injections into the LHC if the difference between the beam trajectory and its reference exceeds a given threshold. During the injection process, rare but heavy losses are expected that will be associated to either bad beam conditions at the end of the transfer line or to injection kicker faults. Most of the beam losses will occur in the TDI. The beam-loss monitors around these devices are part of the LHC beam-loss system described in the beam instrumentation chapter. The position of the intercepting transverse profile monitors is to be surveyed by the SPS software interlock system. Depending on the operation mode of the LHC, the software interlock system should prevent beam extraction when the profile monitors are intercepting the beam to avoid undesired emittance blow-up of the beam. This interlock can, however, be bypassed for machine experiments and during verifications of the transfer line optics.

16.5.6 Post-Mortem System

Bad injections into the LHC may lead to large beam losses or even to magnet quenches. To understand such a sequence of events in detail, the full beam instrumentation data of each injection is made available to the LHC post-mortem system. The position of intercepting beam profile monitors are also provided. The history of beam transfer data, in particular beam losses and beam transmission, will be recorded.

16.6 INTERRELATIONS WITH OTHER MACHINE SYSTEMS

16.6.1 SPS Machine and Transfer Lines

Prior to SPS extraction towards LHC various checks are performed on the circulating beam in the SPS. Should the intensity be too high for the LHC to accept in its present mode of operation or should the beam otherwise not meet the required specifications (number of bunches, synchronisation with respect to the foreseen RF buckets) the beam would not be extracted, unless one of the TED beam dumps in the respective transfer line is in its dump position. If the beam position differs too much from its nominal position, it is not extracted but dumped at the end of the cycle.

The state of critical extraction and transfer line equipment is checked shortly before extraction. If the extraction kickers exhibit any significant flaw, the transfer line collimators are not set properly or the vacuum in the transfer lines is too poor, extraction is inhibited. About 20 ms before transfer the currents in all transfer line power converters are measured, including those of the injection septa. Should one be found outside the tolerance window, extraction will again not take place. Extraction can be inhibited by a signal reaching the extraction kickers until about 1 μs before they would be fired. As already mentioned the injection can be inhibited up to 250 ns before the injection kickers would pulse.

16.6.2 LHC Injection Modes

Injecting beam with significant intensity into the LHC can cause severe damage to equipment if one of the critical LHC elements has wrong settings or is in a faulty state. Since it is not possible to observe the resulting losses and to dump the injected beam in less than several turns, typically a minimum of 3 turns, existing safety systems cannot prevent such damage.

A rigorous application of a succession of different injection modes has to be followed in order to increase progressively the beam intensity from a pilot bunch up to a nominal beam. The different injection related operation modes are injection inhibit, inject-and-dump, inject-and-probe, inject-and-dump with an intense beam and inject-and-fill [36].

Inject-and-dump mode permits a pilot beam to be injected and then dumped very early, i.e. within a few turns up to a few tens of milliseconds. This operation mode requires an automatic dump action with a given delay relative to the LHC injection pre-pulse. If the delay is set to its minimum value, the beam will be dumped during its first turn.

Inject-and-probe mode is based on continuous real-time measurements of the current of the LHC and SPS circulating beams and information on what beam intensity the LHC is permitted to receive. Correlations between the two beams are made in order to enable or disable the injection inhibit as listed in Tab. 16.5. The general rule is that a low intensity beam must first be present in the machine before a higher intensity beam can be injected.

Inject-and-fill mode is synchronised with the abort gap frequency as explained in Chap. 17. A gating-off mechanism for injection is implemented in order to avoid filling the beam abort gap with an unsynchronised injection. The filling pattern and the longitudinal beam position during filling is entirely defined by the radiofrequency system through the timing of the injection pre-pulses sent to the injection kickers.

Table 16.5: Injection conditions in “Inject-and-Probe” mode

Beam Intensity in SPS	Beam Intensity in LHC	LHC Injection Inhibit
Pilot Bunch	None	No
Pilot Bunch	Pilot Bunch	No
Intense Beam	None	Yes
Intense Beam	Pilot Bunch	No
Intense Beam	Intense Beam	No

16.6.3 Control System

The injection kicker control system is fully integrated in the LHC controls infrastructure following the standard controls framework. Integration of the different control entities described above is based on dedicated equipment servers implementing the required functionalities through standard communication contracts and low-level threads.

Operational settings management like kick delay, kick length and kick strength is performed at the application layer through accelerator wide standard application programs. Equipment settings management, such as fine timing delay or interlock thresholds are managed by the equipment experts.

The injection kickers are linked to the machine post-mortem system for correlation of injection related data with other accelerator processes in case of faults. Typical signals acquired are the magnet current pulse shape, the currents of the injected and circulating beams, and the beam permit and beam abort gap signals. Triggering of the post-mortem system will be based on the opening of the beam permit loop. The same signals are also acquired and analysed on a shot-by-shot basis at each injection to continuously monitor the injection kickers with the objective to detect any degradation of their performance.

16.6.4 Radiofrequency

The synchronisation of the injection kicker timing system with the injected and circulating beams is performed at the radiofrequency (RF) level through the generation and the distribution of the fast injection pre-pulse. In order to avoid any modification of the pre-pulse distribution delay, dedicated fibre optics links are used between the RF installation in SR4 and the kicker timing systems installed in UA23 and UA87. Despite the fact that this pre-pulse is locked to the SPS/LHC common frequency, the final longitudinal beam injection position in the LHC also depends on the selected SPS extraction turn. A bad selection of the SPS extraction turn can result in filling the beam abort gap in one shot.

As a fixed phase difference with respect to the revolution frequency exists between the beam abort gap position at the injection kicker and at the dump extraction kicker, the injection kicker timing system can be bound to the extraction kicker synchronisation system through the distribution of the beam abort frequency. On the basis of this beam abort frequency and after compensation of beam time-of-flight and signal distribution delay, a 10.8 μs long gating-off window is included within the injection kicker timing system in order to inhibit the injection pre-pulse if it falls within the window. This window starts 7.8 μs before the beam abort gap at the injection kicker and continues up to the end of the abort gap. If an injected pre-pulse falls within this window, the injection will be inhibited and the arriving beam be sent to the TDI.

16.6.5 Machine Protection System

The injection kicker systems are connected to the LHC beam permit loops and injection into LHC is only enabled when the loops are closed. Opening one of the beam permit loops automatically inhibits the injections with a reaction delay of 250 ns. In this case, the incoming beam is automatically sent to the TDI. The LHC injection inhibit interlock signal is also sent to the SPS extraction interlock in order to inhibit extraction, thus preventing intense beam sent repetitively to the TDI, unless the transfer line dumps are in position to intercept them, for instance in the case of transfer line tests.

16.6.6 Beam Dumping System

At injection, the propagation delays between the beam dumping system and the injection kickers must be taken into account in order to avoid the “1-turn-deadlock”. Opening the beam permit loop in IR6 will immediately trigger the beam dump and will require ≈100 μs to reach the injection kicker in IR2. If a dump request in IR6 occurs just before a new injection, the circulating beam will be dumped but beam injection will still be allowed during the next 100 μs while the beam dump system is not ready. The full consequences of this “1-turn-deadlock” between beam dumping system and injection kickers still have to be studied in more detail.

16.6.7 Collimator System

As the TDI is normally set to 8.5σ_y at injection it is well in the shadow of the secondary LHC collimators which are positioned at 7.0σ_y. However, if the TDI jaws are closed by about 1σ (about 0.5 mm), or if the secondary collimator settings are opened by a similar amount, the TDI jaws may start to see a significant particle load from the secondary halo. The settings of the injection collimation system and the main LHC collimators are therefore interdependent and special care is needed in their operation to satisfy both machine protection and performance requirements.

The TDI and associated TCLs also limit the amount of beam impacting the LHC collimators in the event of injection kicker failures. For the LHC collimation system, the failure cases 2 and particularly 4, described in 16.4.1, could result in beam impacting on collimator jaws.

REFERENCES

[1] A. Hilaire, V. Mertens, E. Weisse, "Beam Transfer to and Injection into LHC", Proc. EPAC'1998, Stockholm, 1998.

[2] Technical Specification of the Steel Septum Magnets for the LHC Injection and Beam Dumping Systems, CERN, SL-Spec 98-31 (MS), 1998.

[3] S. Bidon et al., "Steel Septum Magnets for the LHC Beam Injection and Extraction", Proc. EPAC'2002, Paris, June 2002.

[4] D. Cornuet, J. Dutour, P. Leclère, "Magnetic Measurements of the Steel Septum Magnet used for Injection: MSIB01", CERN, LHC Project Note 280, 2001.

[5] B. Goddard, CERN-AB/BT, J.M. Jimenez, CERN-AT/VAC, private communication (note in preparation).

[6] M. Gyr, "Expected Magnetic Field Quality of the LHC Septum Magnets Used for Injection (MSI) and for Extraction to the Beam Dump (MSD)", CERN, LHC Project Note 129/rev., 1999.

[7] B. Henrist, CERN-AT/VAC Technical Note (in preparation).

[8] I. Collins, "Room Temperature Beam Vacuum System for the LHC Long Straight Sections", CERN EDMS rev. 0.2, N°339088, 2002.

[9] A. Gerardin, CERN, Report EST/SM/ME 01-05-16.

[10] A. Gerardin, "Scratch Test on an Electro-deposed Copper Layer of a Mumetal Pipe", EST/SM-ME EDMS 349561 16/07/02.

[11] L. Vos, CERN-AB/APB, private communication.

[12] J.M. Jimenez, B. Henrist, "Vacuum Chamber for the Circulating Beams in the LHC Injection and Extraction Septa", under approval (EDMS).

[13] H. Burkhardt, "Do We Need Collimation in the Transfer Lines ?", Proc. LHC Workshop, Chamonix XII, Chamonix, 2003.

[14] H. Burkhardt, B.Goddard, V.Mertens, "Passive Protection Devices in the Transfer Lines to the LHC", Proc. PAC'2003, Portland, 2003.

[15] L. Ducimetière et al., "Design of the Injection Kicker Magnet System for CERN's 14 TeV Proton Collider LHC", Proc. 10th IEEE Int. Pulsed Power Conference, Albuquerque, 1995.

[16] R.L. Gluckstern, L.Vos, B.Zotter, "Shielding Particle Beams by Thin Conductors", CERN-SL-2002-014-AP, 2002.

[17] L. Ducimetière et al., "The LHC Injection Kicker Magnet", Proc. PAC'2003, Portland, 2003.

[18] B. Versolatto, "Procédure de traitement des ferrites en vue de leur utilisation dans un système UHV" , CERN-AT/VAC Note (in preparation).

[19] E. Frick et al., "Fast Pulsed Magnet Systems for Proton and Antiproton Injection into the CERN 400 GeV Proton Synchrotron", Proc. 15th Power Modulator Symposium, Baltimore, 1982.

[20] E. Decailloz, PFN design Department, LCC-Thomson, France, private communication, 1993.

[21] Cadence, 2655 Seely Av., San Jose, CA 95134, USA.

[22] O. Brüning et al., "Impact of and Protection Against Failures of the LHC Injection Kickers", Proc. PAC'1999, New York, 1999.

[23] B. Goddard, "Impact of Injection Kicker Failures", 23th LHC Collimation Working Group Meeting, March 28, 2003.

[24] OASIS, http://project-lhc-cp-sigwg.web.cern.ch/project-lhc-cp-sigwg/ and http://ab-co-fc.web.cern.ch/ab-co-fc/AnalogSignals/nAos_for_TT40/main.htm.
[25] P.R. Sala, S. Péraire, “Conceptual Optimisation of the TDI and TCDD Protections for LHC Injection Lines”, CERN AB-Note-2003-059 ATB, 2003.
[26] P. Chiaggiato, CERN-EST/SM, Report on BN Outgassing Measurements, 2001.
[27] A. Fassò et al., “FLUKA: Present Status and Future Developments”, Proc. Int. Conf. On Calorimetry in High Energy Physics, La Biodola (Is. D’Elba), Italy, 1993, Eds. A.Menzione and A.Scribano, World Scientific.
[28] L. Massidda, F. Mura, “Thermal and Mechanical Analyses of the LHC Injection Beam Stopper (TDI)”, CRS4 – Centre for Advanced Studies, Research and Development, Cagliari, Italy, 2003.
[29] M. Meddahi, “Instrumentation Needs for LTI”, Proc. LHC Workshop, Chamonix XI, CERN-SL-2001-003 DI.
[30] J. Wenninger, “Instrumentation for the TI 2 and TI 8 Transfer Lines”, Engineering Specification, EDMS Document LHC-B-ES-0004.
[31] G. Ferioli et al., “Protection and Diagnostic Systems for High Intensity Beams”, CERN-SL-2000-032-BI.
[32] J. Bosser, G. Ferioli, “Comparative Test Results of Various Beam Loss Monitors in Preparation for LHC“, Proc. DIPAC’99, Chester, 1999.
[33] G. Ferioli, “Beam Profile Measurements at 40 MHz in the PS to SPS Transfer Channel”, CERN SL-99-043 BI.
[34] Minutes of the 25th BI LHC/CNGS Technical Board.
[35] J.J. Gras et al., “AB Front End Common Software Architecture”, https://edms.cern.ch/file/380278/1/FEComSA_TC.pdf.
[36] E.C arlier, “Safe Injection into LHC”, Proc. LHC Workshop, Chamonix XII, Chamonix, 2003.